Table V. Summary of Crystallographic Data

	$[(CH_3C_5H_4Mo(\mu\text{-}S))_2S_2CH_2]_2\text{-}(SO_3CF_3)_2$	$[(CH_3C_5H_4Mo(\mu\text{-}S))_2S_2CH_2]_2(BF)_2$
fw	1282.9	1158.4
space group	$C2/c$	$P2_1/n$
a, Å	35.498 (10)	11.476 (5)
b, Å	14.823 (7)	13.843 (6)
c, Å	17.246 (5)	12.577 (4)
β, deg	115.51 (2)	112.97 (3)
V, Å^3	8190 (5)	1839.6 (13)
ρ(calcd), g cm^{-3}	2.081	2.091
radtn	Mo Kα (λ = 0.71073 Å)	Mo Kα (λ = 0.71073 Å)
temp, °C	−35	22–24
2θ range, deg	5.0–50.0	3.0–45.0
scan type	ω	Wyckoff
scan speed, deg min^{-1}	variable; 4.00–60.00	fixed; 4.00
scan range	from 0.80° below 2θ for Kα_1 to 0.80° above 2θ for Kα_2	0.60°
index ranges	$-42 \le h \le 42$	$-12 \le h \le 12$
	$0 \le k \le 17$	$-14 \le k \le 14$
	$-20 \le l \le 20$	$-13 \le l \le 12$
rflctns coll	15266	2964
unique rflctns	7225	2407
obsd rflctns	5714	1487
abs corr	semiempirical	none
min/max transm	0.6265/0.9020	
R, %	6.05	8.73
R_w, %	9.00	11.01

occupied three positions in the asymmetric unit: one was located about two different positions along the 2-fold axis, i.e., at 0, 0.32, $^3/_4$ and at 0, 0.04, $^3/_4$; and the other was at an independent position in the cell. Several different orientations for each of these triflates were found in difference maps. These were included as constrained groups in further least-squares calculations.

Because of the problems with the triflate anions, crystals of the tetrafluoroborate salt were synthesized and examined. After three crystals were mounted, all of which exhibited split peaks, a crystal was located that, while still showing split peaks, was of better quality than the previous ones. A fast data collection on this sample gave data of sufficient quality to confirm a tetranuclear structure similar to that determined for the triflate salt. Numerous attempts to obtain better crystals of the tetrafluoroborate salt were unsuccessful.

Further attempts were therefore made to improve the treatment of the disordered anions in the triflate salt. Several other orientations were added, but there was still significant electron density in the region of two of the triflates. Eight of these peaks were included in the final least-squares cycles as individual atoms rather than as constrained atoms in complete triflates. No further attempts to improve the quality of the structure seemed warranted since the tetranuclear nature of the dication had been established. Hydrogen atoms were not seen in the difference maps, so they were not included. For the final refinement, all methylcyclopentadiene groups were treated as rigid groups and all complete triflates were refined with distance restraints.

Acknowledgment. Support of this work by the National Science Foundation and, in part, by the National Institutes of Health is gratefully acknowledged.

Supplementary Material Available: For the triflate and tetrafluoroborate salts of **1b**, tables of crystal data and collection, solution, and refinement details, atomic coordinates and equivalent isotropic displacement parameters, complete bond distances and angles, and anisotropic displacement parameters (23 pages); listings of observed and calculated structure factors (35 pages). Ordering information is given on any current masthead page.

NMR and X-ray Studies of Penta- and Hexaborane Alkyl Derivatives Involving [3.3.1] and [3.3.2] Ring Systems

Gary M. Edvenson, Donald F. Gaines,* Holly A. Harris, and Charles F. Campana

Department of Chemistry, University of Wisconsin—Madison, Madison, Wisconsin 53706

Received June 15, 1989

The reaction of the $B_5H_8^-$ anion with *B*-chloro-9-borabicyclo[3.3.1]nonane (*B*-Cl-9-BBN) produces a boron bridge substituted *nido*-pentaborane, (μ-9-BBN)B_5H_8 (**1**). The solid-state structure of **1** reveals that the 9-BBN fragment retains its characteristic chair–chair conformation. In solution at room temperature the 9-BBN fragment rotates relative to the pentaborane framework. From a dynamic ^{13}C NMR experiment the free energy of activation for the rotation has been found to be 14.6 ± 0.1 kcal mol^{-1}. In diethyl ether solution this compound slowly converts to a *nido*-hexaborane derivative, 4,5-(cycloocta-1,5-diyl)B_6H_8 (**2**), in which the bridging boron atom has moved into the cluster. The result is the conversion of the [3.3.1] ring system of 9-BBN to a [3.3.2] bi-cycle in which two adjacent basal boron atoms of a *nido*-hexaborane cluster provide the two-atom bridge. Compound **2** is the first example of a fused borane cluster–organic bi-cycle. The solid-state structure of **2** reveals a chair–boat conformation for the [3.3.2] bicyclic ring system. In addition, two independent molecules are observed that differ primarily in the placement of the hydrogen atoms bridging the basal edges of the hexaborane fragment. Compounds **1** and **2** were characterized by ^{11}B, ^{13}C, ^1H, and ^{11}B–^{11}B COSY NMR spectroscopic studies and by single-crystal X-ray diffraction. Crystal data for **1**, $C_8H_{22}B_6$, at −150 °C: triclinic, space group $P\bar{1}$, a = 9.427 (2) Å, b = 10.380 (2) Å, c = 12.525 (2) Å, α = 87.341 (16)°, β = 80.729 (15)°, γ = 89.86 (2)°, Z = 4. Crystal data for **2**, $C_8H_{22}B_6$, at −125 °C: orthorhombic, space group $P2_12_12_1$, a = 9.077 (3) Å, b = 11.585 (3) Å, c = 22.352 (6) Å, Z = 8.

Introduction

As part of our effort to gain a better understanding of the alkylation of pentaborane(9), B_5H_9 we have begun investigating reactions involving the diverse and rapidly growing number of organoborane reagents. The *B*-chloro derivative of commercially available 9-BBN, 9-borabicyclo[3.3.1]nonane, has led to the synthesis of a pentaborane derivative in which the 9-BBN boron atom bridges a pentaborane basal edge. This cluster undergoes a Lewis-base-catalyzed isomerization to a unique molecule in

0276-7333/90/2309-0401$02.50/0 © 1990 American Chemical Society

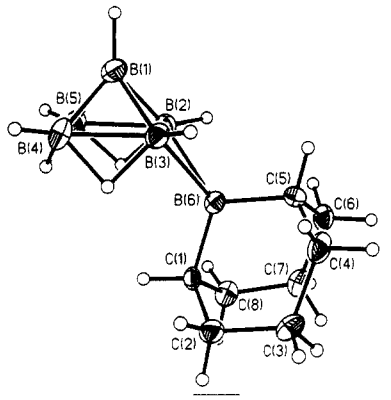

Figure 1. Structure of one of the two independent molecules of $(\mu$-9-BBN)B_5H_8 (1) with thermal ellipsoids at the 30% probability level.

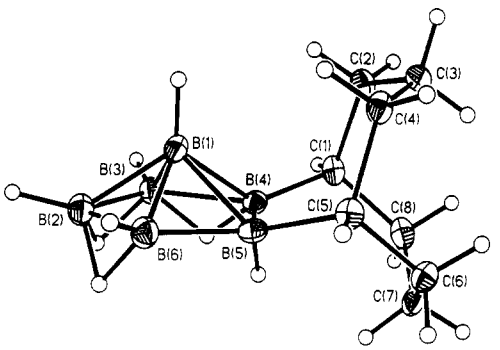

Figure 2. Structure of one of the two independent molecules of 4,5-(cycloocta-1,5-diyl)B_6H_8 (2) with thermal ellipsoids at the 30% probability level.

which a bicyclic ring system and a hexaborane cluster are fused.

The preparation of these compounds may be viewed from several different perspectives. First, this system is an example of the alkylation of penta- and hexaborane.[1,2] Second, it can be viewed as a boron insertion reaction leading to cluster expansion,[3] and third, one can consider the transformation of the 9-BBN moiety that takes place. This paper describes the synthesis, characterization, and some interesting structural features of the penta- and hexaborane derivatives formed.

Synthesis and Spectroscopic Studies

^{11}B, ^{13}C, and ^1H NMR chemical shift data for 1 and 2 are compiled in Table I. The structures of 1 and 2 with the numbering system used, showing thermal ellipsoids at the 30% probability level for non-hydrogen atoms, are shown in Figures 1 and 2, respectively.

$(\mu$-9-BBN)B_5H_8 (1). When a solution of *B*-Cl-9-BBN (3) and the metal pentaborate(1−) MB_5H_8 (M = Li, Na, K) are frozen in contact with one another and warmed to room temperature with stirring, a metathesis reaction occurs, leading to the formation of $(\mu$-9-BBN)B_5H_8 (1) in good yield (eq 1).

$$MB_5H_8 + B\text{-Cl-9-BBN} \rightarrow (\mu\text{-9-BBN})B_5H_8 + MCl \quad (1)$$

M = Li, Na, K

Table I. NMR Data[a] for $(\mu$-9-BBN)B_5H_8 (1) and 4,5-(cycloocta-1,5-diyl)B_6H_8 (2)

^{11}B NMR[b]		^1H NMR[c]		^{13}C NMR[c]	
		$(\mu$-9-BBN)B_5H_8			
B(1)	−38.13 (172)	H(μ3-4,μ5-2)	−2.05	C(3,7)	23.87
B(4,5)	−10.39 (144)	H(μ4-5)	−1.44	C(2,8) or C(4,6)	35.60
B(2,3)	−5.73 (144)	H(1)	1.25	C(4,6) or C(2,8)	36.54
B(6)	+104.00	H(2,3) or H(4,5)	2.66	C(1,5)	38.42
		H(4,5) or H(2,3)	2.84		
		H-C[d]	1.4–2.3		
		4,5-(cycloocta-1,5-diyl)B_6H_8			
B(1)	−50.21 (146)	H-μ	−1.01	C(3) or C(7)	22.04
B(3,6)	+8.52 (146)	H(1)	−0.52	C(7) or C(3)	25.22
B(2)	+12.48 (146)	H(3,6)	3.83	C(2,4) or C(6,8)	27.28
B(4,5)	+26.27	H(2)	4.25	C(6,8) or C(2,4)	31.34
		H-C[d]	1.3–2.1		

[a] All spectra were recorded at 298 K. [b] Chemical shifts in ppm relative to external $BF_3 \cdot OEt_2$, 0 ppm. Values in parentheses are coupling constants, J_{B-H}, in Hz for terminal hydrogens. [c] Chemical shifts in ppm relative to internal methylene chloride-d_2 for 1 and toluene-d_8 for 2. [d] The methylene and methyne hydrogens gave rise to broad resonances in the reported regions.

Compound 1 is a colorless, crystalline material with a melting point slightly above room temperature and is isolated by vacuum sublimation and condensation in a 0 °C U-trap.

In the ^{11}B NMR spectrum of 1 the apical boron, B(1), resonates at −37 ppm, 16 ppm downfield from the apical resonance of B_5H_9. This type of downfield shift was also observed for the apical boron in $(\mu$-$(CH_3)_2B)B_5H_8$.[4] The bridging boron atom, B(6), has no hydrogen substituents and resonates as a singlet at +104 ppm. This very low field chemical shift indicates that B(6) is in a trigonal coordination environment and contributes an sp^2 hybrid oribital to a three-center–two-electron bond with B(2) and B(3). A two-dimensional ^{11}B–^{11}B COSY experiment[5] provides support for the structure shown in Figure 1 and allows the basal resonances to be unambiguously assigned. In the 2-D experiment the only cross peak for the B(6) resonance at +104 ppm is to the resonance at −6 ppm. The latter can thus be assigned to the adjacent equivalent basal boron atoms, B(2,3). The ^{11}B–^{11}B COSY experiment also reveals cross peaks indicating coupling between B(2,3) and B(4,5), between B(2,3) and B(1), and between B(4,5) and B(1). Although the observation of cross peaks between hydrogen-bridged borons has not been commonly observed, we have previously shown[5b] that cross peaks between hydrogen-bridged borons in several medium-sized boron hydrides are readily observed. The presence of cross peaks between the hydrogen-bridged borons in 1 and 2 is consistent with our earlier observations.

The ^{13}C NMR spectrum reveals an interesting temperature dependence. A selected portion of the spectrum over the temperature range studied is shown in Figure 3. At −31 °C, in CD_2Cl_2, two signals are observed for the bridgehead carbons, C(1) and C(5). On this basis the low-temperature orientation of the 9-BBN moiety must be one in which these carbons are inequivalent, as shown in Figure 1, one being below and one directed away from the pentaborane(9) framework. As the temperature is raised, the C(1) and C(5) resonances coalesce, indicating that the 9-BBN moiety is rotating about the boron sp^2-hybridized orbital that bonds it to the pentaborane(9)

(1) Onak, T. *Organoborane Chemistry*; Academic Press: New York, 1975; pp 196–206.
(2) Grassberger, M.; Köster, R. In *Houben-Weyl Methoden der Organischen Chemie*, 4th ed.; Köster, R., Ed.; Thieme: Stuttgart, FRG, 1984; Vol. XIII/3c, pp 96–109.
(3) (a) Shore, S. G. In *Boron Hydride Chemistry*; Muetterties, E. L., Ed.; Academic Press: New Yor, 1975; Chapter 3. (b) Beall, H. *Ibid.*, Chapter 9.
(4) Gaines, D. F.; Iorns, T. V. *J. Am. Chem. Soc.* **1970**, *92*, 4571–4574.
(5) (a) Venable, T. L.; Hutton, W. C.; Grimes, R. N. *J. Am. Chem. Soc.* **1984**, *106*, 29–37. (b) Gaines, D. F.; Edvenson, G. M.; Hill, T. G.; Adams, B. R. *Inorg. Chem.* **1987**, *106*, 1813–1816.

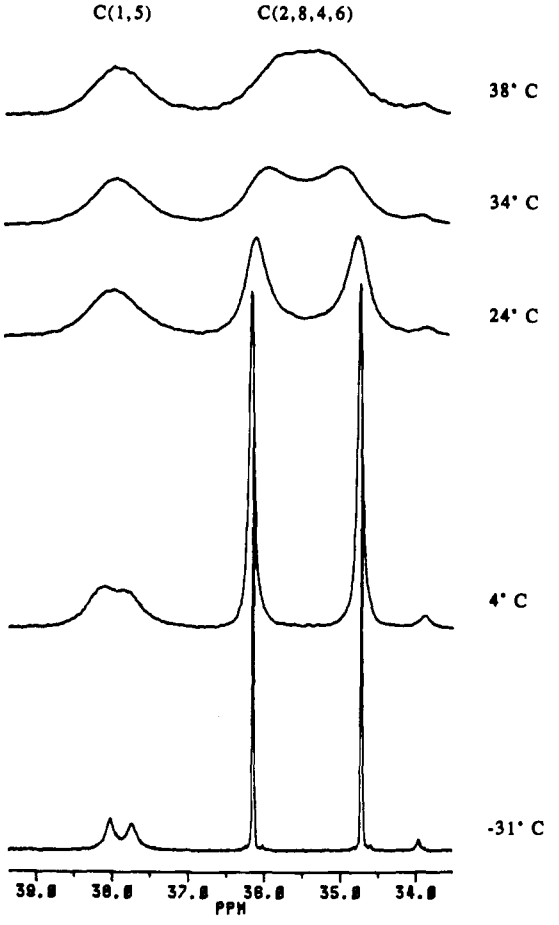

Figure 3. Selected portion of 125-MHz variable-temperature ^{13}C NMR spectra of (μ-9-BBN)B_5H_8 showing the coalescence that occurs on warming between the C(1) and C(5) and between the C(2,8) and C(4,6) resonances. Each of the pairs of coalescing singlets is the result of two-site exchange produced by rotation of the 9-BBN moiety about the axis of the boron sp^2 orbital that bonds it to the B_5H_8 framework.

framework. The C(4,6) and C(2,8) resonances also coalesce, but at a higher temperature due to a greater difference in the chemical shifts. The nature of the C(3,7) resonance does not change significantly with temperature. At low temperatures the C(3) and C(7) carbons are equivalent, giving rise to a sharp resonance. At higher temperatures the rotation of the bicyclic ring leads to a slight broadening of the C(3,7) resonance. In a dynamic NMR experiment the coalescence temperature for the C(4,6) and C(2,8) resonances was determined to be 311.2 K (38.2 °C). At this temperature the rate constant for the internal rotation of the 9-BBN moiety was calculated to be 368 s^{-1} by using the approximate equation $k_c = \pi\delta\nu/2^{1/2}$. This expression has been found to be of satisfactory accuracy, provided that $\delta\nu$ is much larger than the bandwidth in the absence of exchange,[6] a requirement that is met in the present case. The free energy of activation for the rotation at the coalescence temperature, $\Delta G^{\ddagger}_c$, was calculated to be 14.6 ± 0.1 kcal mol^{-1} by using the Eyring equation with a transmission coefficient of 1. An examination of this rotation with use of molecular models reveals that if the B(6)–B(2,3) distance is maintained the closest interaction between the methyne hydrogens on C(1) and C(5) and the terminal hydrogens on B(2) and B(3) is 1.71 Å. This steric interaction provides the most likely major contribution to the barrier to 9-BBN rotation in 1.

(6) Kost, D.; Carlson, E. H.; Raban, M. *J. Chem. Soc. D* **1971**, 656–657.

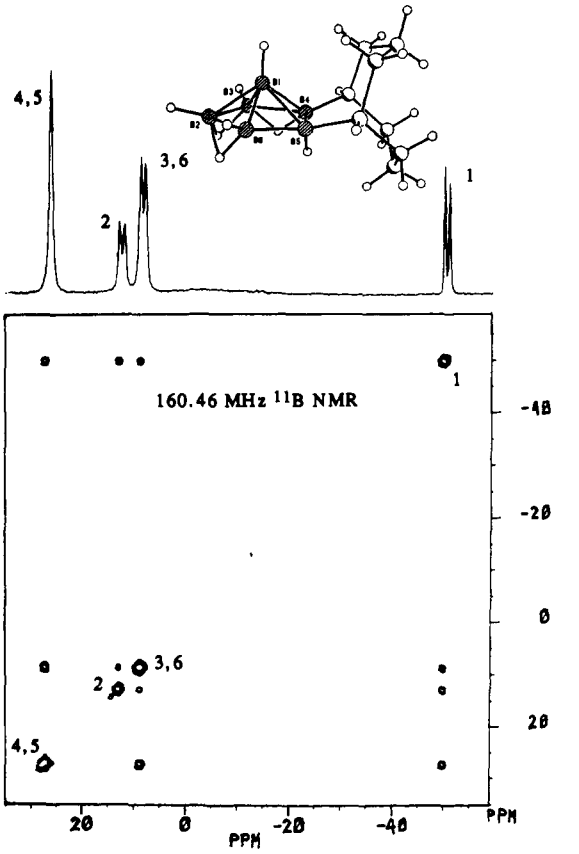

Figure 4. 2-D ^{11}B–^{11}B COSY spectrum of **2** recorded at 22 °C and 160.46 MHz in Et_2O. The 1-D ^{11}B (^1H coupled) spectrum is plotted above the 2-D contour plot as an aid in identifying the resonances on the diagonal and interpreting the cross peaks in the 2-D spectrum (see text). At room temperature the four bridge hydrogens are fluxional on the NMR time scale and give rise to C_s symmetry.

The three bridge hydrogens of **1** are static on the NMR time scale, giving rise to two resonances in the ^1H NMR spectrum with a 2:1 intensity ratio. Terminal hydrogens on boron are found in a 2:2:1 ratio, reflecting the same symmetry evident in the ^{11}B NMR spectrum. The hydrogens of the bicyclic ring give rise to a complex series of resonances from 1.4 to 2.3 ppm.

4,5-(cycloocta-1,5-diyl)B_6H_8 (2). In diethyl ether at room temperature over a period of several weeks **1** is converted to **2** in ~90% yield based on **1**. As observed by ^{11}B NMR spectroscopy, this fascinating conversion proceeds smoothly with no evidence of an intermediate species. The remaining 10% of **1** is involved in an ether-cleavage side reaction, leading to pentaborane(9) and several *B*-alkoxy-9-BBN derivatives. Colorless, crystalline **2** is isolated by vacuum sublimation and condensation in a 0 °C U-trap. In the conversion process the boron atom of 9-BBN that was bridging an edge of the square-based pyramid has been inserted into the cluster to form a pentagonal pyramid. A boron–carbon bond in the original bi-cycle has been broken and re-formed at a boron adjacent to the inserted boron. The result is an enlargement of the bi-cycle from a [3.3.1] to a [3.3.2] system with the two-atom loop being comprised of two borons in the hexaborane basal plane. This is the first example of a fused borane cluster–organic bi-cycle. It appears to be stable indefinitely at room temperature in the absence of air and moisture and reacts only very slowly with water.

The one-dimensional ^{11}B (^1H coupled) NMR spectrum together with the 2-D ^{11}B–^{11}B COSY spectrum of **2** is shown in Figure 4. The 1-D spectrum shows resonances

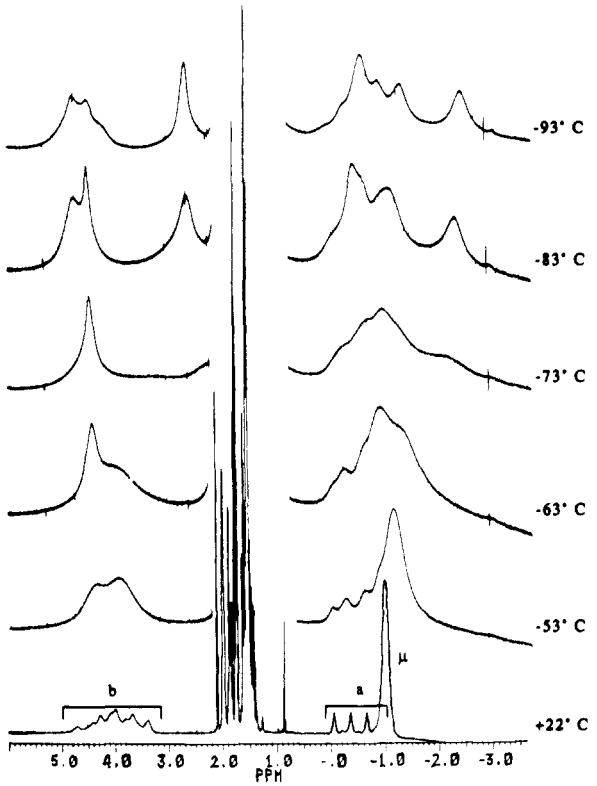

Figure 5. Variable-temperature ^1H NMR spectra (500 MHz) of 4,5-(cycloocta-1,5-diyl)B_6H_8 showing the dynamic behavior of the lower field basal terminal hydrogens and the higher field bridge hydrogens. In the 22 °C spectrum b = basal terminal hydrogens, a = apical terminal hydrogen, and μ = basal bridge hydrogens. The broadening of the apical resonance on cooling results from thermal decoupling.

for one apical and five basal (intensity 2:1:2) borons in regions characteristic of hexaborane(10) derivatives. The lowest field basal resonance of intensity 2 at +26.27 ppm is a singlet, indicating a non-hydrogen substituent, and thus we condluded that **2** was a dialkyl hexaborane(10) derivative. In addition, we presumed that this disubstitution pattern was the result of a cyclooctyl ring bonded by two carbons to adjacent borons, as shown in Figure 2. However, the C_s symmetry implicit in the 1-dimensional ^{11}B NMR spectrum will also allow for a nonadjacent placement of substituents. Thus, the resonance at +26.27 ppm could be assigned to either B(3,6) or B(4,5). The 2-D ^{11}B–^{11}B COSY spectrum of **2** provides the connectivity information needed for an unambiguous assignment. The resonance for the substituted borons at +26.27 ppm shows a cross peak to the basal resonance of intensity 2 at +8.52 ppm but not to the unique basal resonance at +12.48 ppm. This means that the substituted borons are not adjacent to the unique basal boron atom B(2) and therefore can be assigned as B(4,5). The rest of the 2-D spectrum is consistent with this assignment. The doublet basal resonance of intensity 2, B(3,6), shows cross peaks to both B(4,5) and B(2), and all of the basal resonances show cross peaks to the apical boron resonance. This pattern of cross peaks also confirms the pentagonal-pyramidal framework of a hexaborane derivative since the basal borons are found to be interconnected and are all adjacent to the apical boron.

The room-temperature ^1H NMR spectrum of **2** is shown in the lower trace of Figure 5. The resonances for the terminal hydrogens are 1:1:1:1 quartets due to spin coupling with ^{11}B ($I = {}^3/_2$). The two overlapping lower field quartets of intensity 1:2 are assigned to the three basal terminal hydrogens, and the high-field quartet of intensity 1 which overlaps with the bridge hydrogen resonance is assigned to the apical terminal hydrogen (see Table I). The four bridge hydrogens distributed over five basal edges show fluxional behavior on the NMR time scale and give rise to a single averaged resonance at −1.01 ppm. As the temperature is lowered, the terminal basal hydrogens and eventually the terminal apical hydrogen become thermally decoupled from the boron nuclei. Below −53 °C several fluxional processes are quenched at approximately the same rate for both the basal terminal and bridge hydrogens. Figure 5 shows several coalescing resonances in the −93 to −83 °C range and several more in the −83 to −63 °C range. Related dynamic behavior has been observed for B_6H_{10} and 2-MeB_6H_9.[7] The presence of more than one isomer in solution at −93 °C can be inferred from the fact that at least four resonances are observed for the three terminal hydrogens and at least five resonances for the four bridge hydrogens. These additional resonances indicate that the fluxional bridge hydrogens and the unbridged basal edge are not always freezing out in the same location, thus giving rise to molecules with different symmetries and different ^1H chemical shifts. The different low-temperature isomers and the location of the bridge hydrogens will be discussed further in connection with the solid-state structure.

The ^{13}C NMR spectrum of **2** shows four methylene carbons, corresponding to the C(2,4), C(6,8), C(3), and C(7) carbon atoms. As often occurs in organoboranes, the carbons adjacent to boron, C(1,5), are not observed[8] due to excessive broadening, which is presumed to be caused by their scalar interaction with the quadrupolar boron nuclei.[9] Indeed, we were fortunate to observe the C(1) and C(5) resonances in the 9-BBN derivative **1**.

Prior to verification by X-ray diffraction (vide infra), we proposed the structure for **2** shown in Figure 2 on the basis of the previously observed insertion of the bridging boron in (μ-Me_2B)B_5H_8 to give the dimethylhexaborane derivative 4,5-$Me_2B_6H_8$.[4] In fact the present work was undertaken in part to determine whether kinetic or steric constraints of the relatively stable bicyclic 9-BBN moiety would effect such an insertion process.

In many reactions involving the 9-BBN moiety, the B–C bonds remain intact. However, the B–C bond of certain 9-BBN derivatives can be cleaved, for example, by bromine in the presence of water,[10] by acetic acid,[11] and by a base-induced reaction with dichloromethyl methyl ether.[12] The present work indicates that when it is assisted by diethyl ether the pentaborane(9) fragment can also cleave B–C bonds in a 9-BBN ring system. To date, no detailed mechanistic studies of this rearrangement have been undertaken.

Solid-State Structures

The structures of (μ-9-BBN)B_5H_8 (**1**) and 4,5-(cycloocta-1,5-diyl)B_6H_8 (**2**) shown in Figures 1 and 2 were generated from the X-ray-determined solid-state structures. Selected bond distances, bond angles, and fractional coordinates are listed in Tables II–V. Summaries of crystallographic data are given in Table VI.

(μ-9-BBN)B_5H_8 (1). Solution and refinement of the X-ray diffraction data confirmed the 9-BBN-bridged

(7) Brice, V. T.; Johnson, H. D., II; Shore, S. G. *J. Chem. Soc., Chem. Commun.* **1972**, 1128–1129.
(8) Blue, C. D.; Nelson, D. J. *J. Org. Chem.* **1983**, *48*, 4538–4542.
(9) Wrackmeyer, B. *Polyhedron* **1986**, *5*, 1709–1721.
(10) Brown, H. C.; DeLue, N. R. *Tetrahedron Lett.* **1977**, *35*, 3007–3010.
(11) Brown, H. C.; Murray, K. J. *Tetrahedron* **1986**, *42*, 5497–5504.
(12) Carlson, B. A.; Brown, H. C. *Synthesis* **1973**, 776–777.

Table II. Selected Bond Distances (Å) and Angles (deg) for the Ordered Molecule of (μ-9-BBN)B_5H_8

Bond Distances			
B(1)-H(1)	1.085 (39)	B(1)-B(2)	1.676 (6)
B(1)-B(3)	1.676 (5)	B(1)-B(4)	1.676 (6)
B(1)-B(5)	1.682 (5)	B(2)-H(2)	1.113 (41)
B(2)-B(3)	1.707 (5)	B(2)-B(5)	1.803 (5)
B(2)-B(6)	1.878 (5)	B(2)-H(25)	1.337 (31)
B(3)-B(4)	1.799 (5)	B(3)-B(6)	1.917 (5)
B(4)-H(4)	1.042 (38)	B(4)-B(5)	1.788 (6)
B(4)-H(34)	1.317 (31)	B(4)-H(45)	1.326 (29)
B(6)-C(1)	1.562 (4)	B(6)-C(5)	1.558 (4)
C(1)-C(2)	1.542 (4)	C(1)-C(8)	1.538 (4)
C(2)-C(3)	1.523 (4)	C(3)-C(4)	1.524 (4)
C(4)-C(5)	1.553 (4)	C(5)-C(6)	1.533 (5)
C(6)-C(7)	1.526 (4)	C(7)-C(8)	1.522 (4)
Bond Angles			
B(2)-B(1)-B(3)	61.2 (2)	H(1)-B(1)-B(4)	137.3 (22)
B(2)-B(1)-B(4)	96.3 (3)	H(1)-B(1)-B(5)	124.6 (19)
B(2)-B(1)-B(5)	64.9 (2)	B(4)-B(1)-B(5)	64.3 (2)
B(1)-B(2)-H(2)	127.3 (20)	B(1)-B(2)-B(3)	59.4 (2)
H(2)-B(2)-B(5)	137.0 (18)	B(3)-B(2)-B(5)	91.8 (2)
H(2)-B(2)-B(6)	89.4 (19)	B(5)-B(2)-B(6)	124.9 (2)
B(1)-B(3)-B(6)	121.5 (3)	B(2)-B(3)-B(6)	62.1 (2)
H(3)-B(3)-B(6)	97.1 (21)	H(3)-B(3)-H(34)	116.3 (23)
B(6)-B(3)H(34)	89.0 (15)	H(4)-B(4)-B(5)	135.8 (19)
B(1)-B(4)-H(45)	99.8 (13)	B(3)-B(4)-H(45)	108.6 (13)
B(2)-B(5)-B(4)	88.2 (2)	B(4)-B(5)-H(45)	47.9 (14)
H(25)-B(5)-H(45)	90.1 (21)	B(2)-B(6)-B(3)	53.4 (2)
B(2)-B(6)-C(1)	120.9 (2)	B(2)-B(6)-C(5)	119.8 (2)
C(1)-B(6)-C(5)	111.8 (2)	B(3)-H(34)-B(4)	86.8 (19)
B(4)-H(45)-B(5)	89.8 (18)	B(6)-C(1)-C(2)	107.1 (2)
C(2)-C(1)-C(8)	114.2 (2)	C(1)-C(2)-C(3)	115.2 (2)
C(2)-C(3)-C(4)	114.3 (2)	C(3)-C(4)-C(5)	115.3 (2)

Table III. Fractional Coordinates for the Ordered Molecule of (μ-9-BBN)B_5H_8 (1)

atom	10^4x	10^4y	10^4z	10^4U,[a] Å^2
B(1)	3491 (4)	6224 (4)	4037 (3)	454 (14)
B(2)	2132 (4)	6229 (3)	3324 (3)	363 (12)
B(3)	2063 (4)	7157 (4)	4422 (3)	355 (12)
B(4)	3814 (4)	7816 (4)	3899 (3)	441 (14)
B(5)	3897 (4)	6832 (4)	2757 (3)	387 (13)
B(6)	483 (3)	7252 (3)	3630 (3)	271 (11)
C(1)	215 (3)	8421 (3)	2857 (2)	285 (9)
C(2)	-595 (3)	9448 (3)	3568 (3)	373 (11)
C(3)	-1942 (3)	8967 (3)	4319 (3)	398 (11)
C(4)	-1762 (3)	7680 (3)	4916 (3)	432 (12)
C(5)	-952 (3)	6629 (3)	4216 (2)	353 (10)
C(6)	-1774 (3)	6152 (3)	3348 (3)	412 (11)
C(7)	-1971 (3)	7136 (3)	2441 (2)	388 (11)
C(8)	-619 (3)	7914 (3)	2002 (2)	383 (11)
H(1)	3985 (42)	5376 (38)	4356 (30)	863 (126)
H(2)	1438 (41)	5399 (38)	3205 (29)	805 (117)
H(3)	1467 (37)	7154 (32)	5181 (28)	616 (102)
H(4)	4526 (39)	8412 (34)	4204 (28)	686 (109)
H(5)	4735 (36)	6578 (31)	2087 (26)	585 (97)
H(25)	2687 (37)	6929 (31)	2432 (26)	622 (101)
H(34)	2500 (33)	8279 (29)	3987 (23)	474 (86)
H(45)	3931 (30)	7982 (28)	2833 (23)	397 (80)

[a] For non-hydrogen atoms U is a given as U_{eq}, defined as one-third of the trace of the orthogonalized U_{ij} tensor.

pentaborane structure of 1. The unit cell contains two independent molecules, one of which is well ordered and will be discussed first. In this molecule the 9-BBN moiety is in the orientation shown in Figure 1, which is in agreement with the low-temperature ^{13}C NMR spectrum. The bond lengths and angles within the 9-BBN portion of the molecule are, with a few minor exceptions, within the standard deviations of those reported for the hydrogen-bridged 9-BBN dimer.[13] The bridging boron, B(6), is 1.875 (5) and 1.916 (5) Å from B(2) and B(3), respectively. These distances are about 8% longer than the sum of covalent boron radii and are in the normal range for substituents in bridging positions on B_5H_9.

The C(2),C(4),C(6),C(8) plane is nearly at a right angle (87.6°) to the B(2),B(3),B(6) plane. On the basis of the geometry of 9-BBN, this would suggest that the sp^2 orbital

(13) Brauer, D. J.; Krüger, C. *Acta Crystallogr., Sect. B* **1973**, *29*, 1684-1690.

Table IV. Selected Bond Distances (Å) and Angles (deg) for the Ordered Molecule of 4,5-(cycloocta-1,5-diyl)B_5H_8

Bond Distances			
B(1)-H(1)	1.056 (23)	B(1)-B(4)	1.771 (4)
B(1)-B(5)	1.849 (4)	B(1)-B(6)	1.805 (4)
B(1)-B(2)	1.755 (4)	B(1)-B(3)	1.754 (4)
B(4)-H(45)	1.309 (20)	B(4)-B(5)	1.759 (4)
B(4)-B(3)	1.819 (4)	B(4)-H(34)	1.316 (20)
B(4)-C(1)	1.584 (4)	H(45)-B(5)	1.230 (22)
B(5)-B(6)	1.654 (4)	B(5)-C(5)	1.597 (4)
B(6)-H(6)	1.060 (23)	B(6)-H(62)	1.271 (21)
B(6)-B(2)	1.753 (4)	H(62)-B(2)	1.325 (21)
B(2)-H(2)	1.100 (23)	B(2)-H(23)	1.262 (21)
B(2)-B(3)	1.806 (4)	H(23)-B(3)	1.260 (21)
B(3)-H(3)	1.070 (23)	B(3)-H(34)	1.226 (21)
C(2)-C(3)	1.530 (3)	C(3)-C(4)	1.523 (3)
C(4)C(5)	1.564 (3)	C(5)-C(6)	1.559 (3)
C(6)-C(7)	1.545 (3)	C(7)-C(8)	1.542 (4)
Bond Angles			
H(1)-B(1)-B(4)	122.6 (13)	H(1)-B(1)-B(5)	122.8 (13)
B(4)-B(1)-B(5)	58.1 (1)	B(4)-B(1)-B(6)	102.5 (2)
B(5)-B(1)-B(6)	53.8 (1)	H(1)-B(1)-B(2)	124.1 (13)
B(4)-B(1)-B(2)	108.4 (2)	B(1)-B(4)-H(45)	96.8 (10)
B(1)-B(4)-B(5)	63.2 (2)	H(45)-B(4)-B(5)	44.3 (10)
B(1)-B(4)-B(3)	58.5 (1)	H(45)-B(4)-B(3)	106.8 (10)
B(5)-B(4)-B(3)	107.9 (2)	H(45)-B(4)-H(34)	90.9 (14)
B(5)-B(4)-H(34)	122.3 (10)	B(1)-B(4)-C(1)	132.1 (2)
H(45)-B(4)-C(1)	118.8 (10)	B(5)-B(4)-C(1)	121.7 (2)
B(3)-B(4)-C(1)	128.0 (2)	B(4)-H(45)B(5)	87.6 (13)
B(4)-B(5)-C(5)	112.7 (2)	H(45)-B(5)-C(5)	113.7 (10)
B(6)-B(5)-C(5)	133.3 (2)	B(1)-B(6)-H(6)	127.4 (13)
B(5)-B(6)-H(6)	130.8 (13)	B(5)-B(6)-H(62)	112.7 (11)
H(6)-B(6)-H(62)	110.9 (17)	H(6)-B(6)-B(2)	114.8 (13)
B(1)-B(2)-B(6)	61.9 (2)	H(62)-B(2)-H(2)	116.5 (17)
B(4)-B(3)-B(2)	104.1 (2)	H(23)-B(3)-H(34)	99.8 (14)
B(4)-C(1)-C(2)	111.1 (2)	B(4)-C(1)-C(8)	113.5 (2)
C(2)-C(1)-C(8)	111.9 (2)	C(1)-C(2)-C(3)	116.5 (2)
C(2)-C(3)-C(4)	118.6 (2)	C(5)-C(6)-C(7)	119.3 (2)
C(6)-C(7)-C(8)	120.6 (2)		

Table V. Fractional Coordinates for the Ordered Molecule of 4,5-(cycloocta-1,5-diyl)B_6H_8 (2)

atom	10^4x	10^4y	10^4z	10^4U,[a] Å^2
B(1)	7497 (3)	3656 (3)	1103 (1)	278 (9)
B(2)	8625 (3)	3970 (3)	486 (1)	359 (10)
B(3)	6947 (3)	3149 (3)	398 (1)	308 (9)
B(4)	5638 (3)	3868 (2)	889 (1)	259 (8)
B(5)	6541 (3)	5047 (3)	1222 (1)	269 (9)
B(6)	8280 (3)	5075 (3)	1003 (1)	333 (10)
C(1)	4140 (3)	3376 (2)	1147 (1)	287 (7)
C(2)	4363 (3)	2855 (2)	1783 (1)	327 (8)
C(3)	4411 (3)	3713 (2)	2304 (1)	330 (8)
C(4)	5652 (2)	4598 (2)	2322 (1)	321 (8)
C(5)	5712 (2)	5508 (2)	1806 (1)	294 (7)
C(6)	4165 (3)	6041 (2)	1683 (1)	322 (8)
C(7)	3221 (3)	5558 (2)	1165 (1)	348 (8)
C(8)	2856 (3)	4260 (2)	1131 (1)	352 (8)
H(1)	7805 (27)	3105 (21)	1458 (10)	385
H(2)	9689 (24)	3637 (23)	325 (10)	385
H(3)	6873 (29)	2278 (19)	241 (11)	385
H(6)	9231 (25)	5418 (21)	1212 (11)	385
H(23)	7756 (24)	3747 (20)	61 (9)	385
H(34)	5762 (23)	3631 (20)	315 (9)	385
H(45)	5740 (25)	4975 (17)	780 (9)	385
H(62)	8411 (26)	5097 (17)	437 (9)	385

[a] For non-hydrogen atoms U is given as U_{eq}, defined as one-third of the trace of the orthogonalized U_{ij} tensor.

Table VI. Summary of Crystallographic Data for 1 and 2

	1	2
empirical formula	$C_8H_{22}B_6$	$C_8H_{22}B_6$
cryst color and habit	colorless prism	colorless prism
cryst size, mm	0.15 × 0.20 × 0.30	0.20 × 0.20 × 0.20
cryst syst	triclinic	orthorhombic
space group	$P\bar{1}$	$P2_12_12_1$
unit cell dimens		
a, Å	9.427 (2)	9.077 (3)
b, Å	10.380 (2)	11.585 (3)
c, Å	12.525 (2)	22.352 (6)
α, deg	87.34 (2)	
β, deg	80.73 (2)	
γ, deg	89.86 (2)	
V, Å^3	1208.3 (4)	2350.5 (12)
Z, molecules/cell	4	8
wavelength, Å	0.71069	1.54178
temp, °C	−150	−125
abs coeff, mm^{-1}	0.045	0.312
abs corr	none	none
diffractometer	Syntex $P\bar{1}$	Nicolet P3f
scan type	Wyckoff	Wyckoff
2θ range, deg	3–45	3.5–110
index ranges	$\pm h,\pm k,+l$	$\pm h,+k,+l$
no. of measd rflns	3322	3470
no. of indep rflns	3094	2901
agreement between equiv rflns, %	2.27	3.86
weighting scheme (w^{-1})	$\sigma^2(F) + 0.0010F^2$	$\sigma^2(F) + 0.0036F^2$
final R (obsd data), %	6.77	4.61
final R_w (obsd data), %	9.13	6.77
goodness of fit	2.25	1.09

of B(6) that bonds with the pentaborane cluster lies nearly in the B(2),B(3),B(6) plane. Boron atoms B(1), B(2), B(3), and B(6) are essentially in the same plane, the mean deviation from the plane being 0.01 Å. The external dihedral angle between the B(1),B(2),B(3) and B(2),B(3),B(6) planes is 181.6°, while the similarly measured external dihedral angles for the bridge hydrogens range from 189.5° for H(45) to 200.8° for H(34). These values are similar to those found in the two bridge-substituted pentaborane(9) derivatives that have been characterized by single-crystal X-ray diffraction, namely, 1-Br-(μ-Me_3Si)B_5H_7[14] and μ-[η^5-(C_5H_5)Be]B_5H_8.[15] In both of these compounds the external dihedral angle for the bridging heteroatom was found to be close to 180° while that for the bridge hydrogens was between 186 and 202°.

Minor distortions are observed in the pentaborane portion of the molecule. The shortest B(basal)–B(basal) edge is the boron-bridged one, B(2)–B(3), which is 1.707 (5) Å. The other basal edges range from 1.788 (6) Å for B(4)–B(5) to 1.803 (5) Å for B(2)–B(5). This shortening of the bridged edge was also observed for the silicon- and beryllium-bridged[14,15] pentaborane derivatives. The apical terminal hydrogen tilts toward the B(2)–B(5) edge, the B(1)–H(1) bond making an angle of 8.6° with the normal to the basal plane.

The other independent molecule in the unit cell of 1 was found to be disordered in the 9-BBN portion of the structure, with two different orientations being present. Refinement of the occupancies revealed that in 84.2 (5)% of the molecules the orientation of the 9-BBN fragment is similar to that of the other independent molecule (see Figure 1), but in 15.8% of the molecules the 9-BBN fragment is in a skewed orientation. Figure 6 shows that the 9-BBN fragment in these molecules is rotated about the axis between B(6a) and the midpoint of B(2a) and

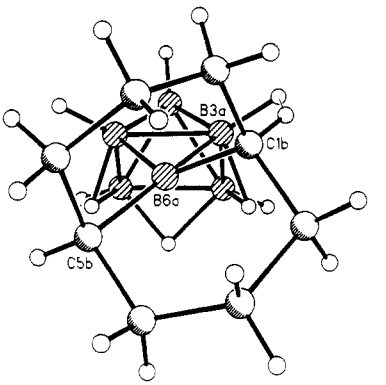

Figure 6. Structure of the disordered molecule of (μ-9-BBN)B_5H_8 (1), showing the skewed orientation of the 9-BBN portion, with a dotted line indicating the close nonbonding interaction between the hydrogens on B(3a) and C(1b).

B(3a) and is also bent 21° away from this axis so that the methyne hydrogen of C(1b) and the terminal hydrogen of B(3a) come within 1.097 Å of each other. A dotted line in Figure 6 designates the extremely close nonbonding interaction between these hydrogens. Another significant distortion in the skewed molecule is shown in the bond lengths between the bridgehead carbons and the bridging boron, which are 1.481 (5) Å for B(6a)–C(1b) and 1.742 (19) Å for B(6a)–C(5b) compared with values of 1.562 (4) and 1.558 (4) Å for the same distances in the other independent molecule. It is not clear why the molecule adopts this distinctly strained conformation.

4,5-(cycloocta-1,5-diyl)B_6H_8 (2). The solid-state structure of **2**, shown in Figure 2, consists of six boron atoms that form a pentagonal pyramid and are bonded at two adjacent basal borons to the C(1) and C(5) carbons of a cyclooctyl ring. The result is a [3.3.2] bicyclic ring system in which adjacent basal hexaborane atoms occupy the two-atom loop between the C(1) and C(5) bridgehead atoms. The bicyclic ring system assumes a chair–boat conformation, the chair part projecting above the hexaborane basal plane and consisting of C(1), C(2), C(3), C(4), C(5), B(5), and B(4) and the boat part projecting below the hexaborane basal plane and consisting of C(1), C(8), C(7), C(6), C(5), B(5), and B(4). The chair–boat conformation has been found to be the most stable in bicyclo[3.3.2]decyl derivatives in which the bridgehead atoms and the two-atom loop are constrained to lie in the same plane,[16–18] as they are in **2**. The nonbonding distance between the hydrogen on C(7) that is directed at the cluster, H(7′), and the bridge hydrogen on the B(4)–B(5) edge, H(45), is 2.06 Å. An examination of molecular models reveals that if the boat conformation was present in the portion of the bi-cycle above the basal plane the distance between the B(1) terminal hydrogen and the methylene hydrogen on C(3) directed at the cluster would be only 1.65 Å. This potentially strong nonbonding interaction is the likely reason for the boat conformation in the portion of the bi-cycle below the basal plane.

The nonbonded repulsion between H(7′) and H(45) is also apparently responsible for the flatness of the boat portion compared to the chair portion of the bi-cycle. This is shown by a dihedral angle for C(1),C(8),C(6),C(5)–C(6),C(7),C(8) of 46.3° compared with a value of 54.4° for

(14) Calabrese, J. C.; Dahl, L. F. *J. Am. Chem. Soc.* **1971**, *93*, 6042–6047.
(15) Gaines, D. F.; Coleson, K. M.; Calabrese, J. C. *J. Am. Chem. Soc.* **1979**, *101*, 3979–3980.
(16) Russel, G. A.; Keske, R. G. *J. Am. Chem. Soc.* **1970**, *92*, 4460–4461.
(17) Murray-Rust, J.; Murray-Rust, P. *Acta Crystallogr., Sect. B* **1975**, *31*, 310–331.
(18) Doyle, M.; Hafter, R.; Parker, W. *J. Chem. Soc., Perkin Trans. 1* **1977**, 364–372.

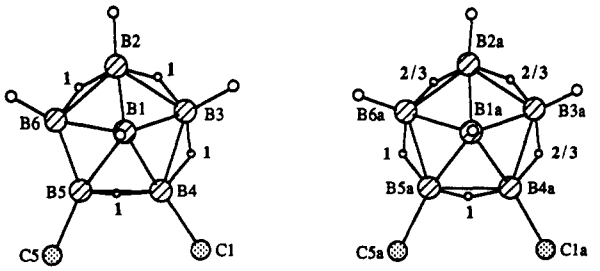

2 2a

Figure 7. View down on the basal plane of the two independent molecules (2 and 2a) of 4,5-(cycloocta-1,5-diyl)B_6H_8 (**2**), showing the bridge hydrogen occupancies in bold numbers.

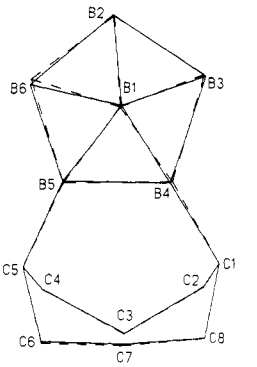

Figure 8. View of the superimposed boron and carbon frameworks of the two independent molecules of 4,5-(cycloocta-1,5-diyl)B_6H_8 (**2**). One (2 of Figure 7) is shown with solid lines and the other (2a of Figure 7) with dashed lines.

the C(1),C(2),C(4),C(5)–C(2),C(3),C(4) dihedral angle.

The angle that the terminal B(4)–C(1) and B(5)–C(5) bonds make with the basal plane is within the normal range of terminal substituents in hexaborane derivatives; however, the cyclooctyl substituent does force these bonds to tilt toward each other slightly. This is shown by the sum of the two angles C(1)–B(4)–B(5) and B(4)–B(5)–C(5), which is 234.4° compared to sums of edge to terminal substituent angles for the other basal edges, which range from 239.4 to 264.1°.

Perhaps the most interesting feature of the solid-state structure of **2** is that one of the two independent molecules in the unit cell has a completely ordered arrangement of bridge hydrogen atoms (molecule 2 in Figure 7). The B(5)–B(6) edge is always unbridged in this molecule and has the shortest B–B distance in the molecule, 1.654 (4) Å. The bond distances in this molecule correspond with what would be expected on the basis of the 4220 topological representation[19] of hexaborane(10) with two-center–two-electron bonds on the B(5)–B(6) and B(1)–B(3) edges. The tautomerism that is responsible for the C_s symmetry of **2** in solution at room temperature has been frozen out in an ordered manner for this molecule of the unit cell at −125 °C.

In the second independent molecule of the unit cell (molecule 2a in Figure 7) the tautomerism has again been frozen out, but in a disordered fashion. Four bridge hydrogens are distributed among the five basal edges. The H(45a) and H(56a) hydrogens each have an occupancy factor of 1, but the bridge hydrogens in the other three positions have occupancy factors of $^2/_3$. Apart from the bridge hydrogens the overall structures of molecules 2 and 2a are very similar, as can be seen from Figure 8, in which the boron and carbon frameworks of the two molecules have been superimposed on each other. The main difference is that as a result of the disorder in molecule 2a less variation is observed for the B–B distances as compared to that in molecule 2.

The largest residual peak for **2** was 0.27 e Å^{-3}, located 1.16 Å from B(3a) and 0.54 Å from H(3a) in molecule 2a (Figure 7). The only residual near the vacant B(5)–B(6) edge in the ordered molecule (2 in Figure 7) was 0.20 e Å^{-3}, located 0.82 Å from B(5) and 1.06 Å from B(6).

A striking feature of the solid-state structure of **2** is that in both independent molecules there is always a bridge hydrogen on the B(4)–B(5) edge and an adjacent edge. The single averaged bridge hydrogen resonance in the room-temperature ^{1}H NMR spectrum of **2** indicates that all of the bridge hydrogens can migrate under these conditions. The fact that bridge hydrogens are always "trapped" on two specific edges as the compound is cooled may have something to do with the mechanism of hydrogen migration in hexaborane(10). According to the mechanism proposed for this rearrangement,[20] a hydrogen migrating from a bridged to an unbridged edge occupies a terminal position on the boron between the two edges in the transition state, thus generating a transient BH_2 group. As **2** is cooled, the size and cyclic nature of the cyclooctyl substituent may prevent the proper transition state for hydrogen migration from being attained on the edges in question. However, this rationale does not explain the 100% occupancy of the B(4)–B(5) edge at low temperatures. What process could allow a bridge hydrogen to migrate into the H(45) position but not migrate out?

The answer to this question may be related to the previously mentioned steric interaction between the H(45) bridge hydrogen and the methylene hydrogen H(7′). At some intermediate temperature before the hydrogen fluxionality is completely frozen out, a bridge hydrogen may be able to migrate from an adjacent edge into the B(4)–B(5) edge, but once under the influence of the nonbonding repulsion from H(7′) it may not be able to achieve the proper geometry for migrating out. The nonbonding repulsion between H(45) and H(7′) does seem to affect the location of H(45). In the first molecule (2 in Figure 7) the dihedral angle that B(4),B(5),H(45) makes with the exterior basal plane is 83.2° compared with 75.8° for H(62),-B(6),B(2), 62.6° for H(23),B(2),B(3), and 60.2° for H-(34),B(3),B(4). In the second molecule (2a in Figure 7) the nonbonding distance between H(45a) and H(7a′) is quite short at 1.96 Å; however, the effect on the H(45a) location is much less pronounced as evidenced by a dihedral angle of 76.2° between H(45a),B(4a),B(5a) and the exterior basal plane.

Although this system is fairly complex, a plausible explanation based on the preceding analysis is that as **2** is cooled the hydrogen fluxionality is quenched in three stages. The first barrier to migration occurs when a bridge hydrogen migrates into the B(4)–B(5) edge and then cannot leave. The second barrier to migration occurs when the cyclooctyl substituent locks up the B(4,5) edge and an edge adjacent to it, and the third stage occurs at the low-temperature limit when hydrogen movement is completely frozen out. The second stage is necessary in order to explain why the occupancy of the non-B(4a)–B(5a) edges in molecule 2a is 1, $^2/_3$, $^2/_3$, $^2/_3$ and not $^3/_4$, $^3/_4$, $^3/_4$, $^3/_4$. Actually it is not necessary for the edge freezing out adjacent to B(4)–B(5) to contain a bridge hydrogen. In fact,

(19) Lipscomb, W. N. *Boron Hydrides*; W. A. Benjamin: New York, 1963.

(20) Lipscomb, W. N. *J. Inorg. Nucl. Chem.* **1959**, *11*, 1–8.

if we assume that the B(5)–B(6) edge in molecule 2 and the B(5a)–B(6a) edge in molecule 2a is the one that preferentially "locks up", then we have a common explanation for the origin of the two independent molecules. In molecule 2 it locks up with the edge vacant and the result is that the fluxionality of the remaining hydrogens is immediately quenched, leading to the ordered structure observed. In molecule 2a the B(5a)–B(6a) edge locks up with a bridge hydrogen present. The remaining two bridge hydrogens continue to migrate on the three nonfrozen edges until their motion is quenched at the low-temperature limit, resulting in a disordered arrangement of bridge hydrogens. This explanation, though speculative, is not inconsistent with the low-temperature ^1H NMR spectra (Figure 5), which were difficult to interpret as a result of large line widths and multiple isomers.

Experimental Section

Standard high-vacuum techniques were used for manipulation and purification of volatile compounds. Other air-sensitive materials were handled in glovebags flushed with dry nitrogen. The ^{11}B, ^{13}C, and ^1H NMR spectra were obtained at 160.46, 125.75, and 500.13 MHz, respectively on a Bruker Instruments Corp. AM 500 spectrometer. The NMR samples were prepared with use of 5 mm o.d. NMR tubes, and lock was achieved with deuterated solvents, except for the 2-D ^{11}B–^{11}B COSY experiments, which were acquired unlocked. Unless otherwise noted, NMR data were collected at ambient temperature and referenced externally to $BF_3{\cdot}OEt_2$ with positive chemical shifts downfield. Acquisition and processing parameters for 2-D ^{11}B–^{11}B COSY experiments involving (μ-9-BBN)B_5H_8 (1) and 4,5-(cycloocta-1,5-diyl)B_6H_8 (2) were as follows: solvent, hexane for 1 and Et_2O for 2; angle for mixing pulse, 45° for 1 and 2; size of data matrix ($t_1 \times t_2$), 256 × 1K for 1 and 128 × 512 for 2; apodization function, Gaussian with LB = −1000 and GB = 0.375 for 1 and unshifted sine-bell function for 2. Processing of the two-dimensional data matrix involved apodization, zero-filling once in t_1, Fourier transformation, and symmetrization.

Pentaborane(9) was from laboratory stock. Sodium hydride, obtained as a 50% dispersion in mineral oil from Aldrich Chemical Co., was used as received. Dimethyl ether was dried over KH and stored over Na, from which it was vacuum distilled as needed. Dichloromethane was dried over P_2O_5 and vacuum distilled as needed. Diethyl ether was dried over and vacuum-distilled from Na/benzophenone. *B*-Cl-9-BBN was prepared by the literature method.[21]

Preparation of (μ-9-BBN)B_5H_8 (1). Typically a solution of 5.0 mmol of NaB_5H_8 was prepared in the usual manner[22] from NaH and B_5H_9 in 5 mL of dimethyl ether in a 100-mL round-bottom reactor equipped with a 12-mm Kontes O-ring stopcock. The reaction vessel was cooled to −196 °C, and the H_2 was pumped out. Five milliliters of dichloromethane was condensed into the flask. Dry N_2 was admitted to the flask, and under a stream of nitrogen 5.0 mL of a 1.1 M solution of *B*-Cl-9-BBN in hexane was syringed slowly into the reaction vessel so as to freeze above the NaB_5H_8 solution. Due to the high air and moisture sensitivity of *B*-Cl-9-BBN the syringe was filled in a glovebag and moved to the reaction vessel with a septum plugging the needle. The reactor was reevacuated, sealed, and warmed to room temperature with stirring over a period of about 20 min. At this point the solution was slightly yellow and white precipitate was present. The volatile components of the vlask were distilled into U-traps maintained at 0 and −196 °C in series. Once the solvents were out of the reactor, the product began condensing in the 0 °C trap as a white solid. Over several days the solid formed colorless crystals. Due to the low volatility of 1 it was necessary to pump on the gray residue in the reactor for several days in order to recover the maximum amount of product. In a separate reaction with 9.9 mmol of NaB_5H_8 and with CH_2Cl_2 and hexane as the solvents, the yield was 1.426 g (7.8 mmol) of 1 (79% based on NaB_5H_8). At room temperature 1 decomposes over a period of months to 9-BBN and unidentified compounds, one of which is deep orange.

Preparation of 4,5-(cycloocta-1,5-diyl)B_6H_8 (2). About 2 mmol of (μ-9-BBN)B_5H_8 (1) was sublimed under a dynamic vacuum into a pump-through 100-mL reactor having two Kontes O-ring stopcocks. Several milliliters of diethyl ether was condensed into the flask, which was then sealed. At the same time an NMR tube containing about 0.05 mmol of 1 and 0.4 mL of diethyl ether was prepared and sealed. The flask and NMR tube were maintained at room temperature. The progress of the reaction was followed by periodic observation of the ^{11}B NMR spectrum of the solution in the NMR tube. After 3 weeks no resonances due to 1 remained. About 90% of the total boron in the solution was present in resonances due to 2 (see Table I). The remainder of the spectrum showed only B_5H_9 and several resonances near +53 ppm characteristic of R_2BOR compounds, attributed to *B*-alkoxy-9-BBN derivatives.

Crystallographic Studies of (μ-9-BBN)B_5H_8 (1) and 4,5-(cycloocta-1,5-diyl)B_6H_8 (2). Crystals of 1 suitable for X-ray diffraction were grown by sublimation in a 0 °C U-trap over a period of days under a dynamic vacuum. A small amount of 2 was sublimed into a 9-mm Pyrex tube, which was then sealed under vacuum. Crystals of 2 suitable for X-ray diffraction grew by sublimation in this tube over a period of several weeks at room temperature. Crystals of 1 and 2 were cut and mounted in X-ray capillary tubes in a nitrogen-filled glovebox. The tubes were flame-sealed under nitrogen outside the box.

The Nicolet SHELXTL PLUS (MicroVAX II) system was used for solution and refinement. The structures of 1 and 2 were solved by direct methods and refined by full-matrix least-squares cycles. The quantity minimized was $\sum w(F_o - F_c)^2$. An extinction correction of $\chi = 0.0042$ (13) was used for 2, where $F^* = F[1 + 0.002\chi F^2/\sin 2\theta]^{-1/4}$. The borane hydrogens of 1 were located via a difference map, and positional and isotropic thermal parameters were refined. A Riding model was used for all of the 9-BBN hydrogens, and isotropic U's were refined except for those hydrogens in the skewed portion of the disordered molecule, for which fixed isotropic U's were employed. The borane hydrogens of 2 were located via a difference map and positionally refined with fixed isotropic U's. A Riding model with fixed isotropic thermal parameters was used for the cyclooctyl hydrogens.

Acknowledgment. We thank Dr. Douglas R. Powell for much advice and help in preparing the crystallographic results for publication. We also thank the National Science Foundation for support of this research and for major instrumentation grants.

Supplementary Material Available: For (μ-9-BBN)B_5H_8 and 4,5-(cycloocta-1,5-diyl)B_6H_8, stereoscopic representations, tables of anisotropic thermal parameters, and complete listings of atomic coordinates, bond distances, and bond angles (16 pages); listings of F_o and F_c values (22 pages). Ordering information is given on any current masthead page.

(21) Brown, H. C.; Kulkarni, S. U. *J. Organomet. Chem.* **1979**, *168*, 281–293.
(22) Geanangel, R. A.; Shore, S. G. *J. Am. Chem. Soc.* **1967**, *89*, 6771–6772.